Overview of Weak Values and Enhancement of Small Signals in Physics and Chemistry

Joseph S. Choi[1, *]

[1] *The Institute of Optics, University of Rochester, Rochester, New York 14627, USA*

(Dated: April 29, 2013)

An overview of quantum weak values is given along with novel experiments that utilized weak value measurement. Weak values is then compared to other enhancements in the field of chemistry for weak chiral signals.

PACS numbers: 42.50.Ct, 33.55.+b, 42.25.Ja, 78.20.Ek

INTRODUCTION

This paper provides a review of what is known as weak value measurement theory, which arose out of the time-symmetric approach to quantum mechanics [1–4]. Experiments using weak values will also be discussed as these have provided a very new perspective for describing measurement and its effects in quantum mechanics [5], as well as high-precision measurements that have increased state-of-the-art precision technology by orders of magnitude [6]. Comparison to techniques used in the field of chemisty in spectroscopy will be provided to explore their similarities with weak values [7].

WEAK VALUE MEASUREMENT

The theory for weak values was first introduced in an attempt to develop a time-symmetric theory for quantum mechanics by Aharonov, Bergmann, and Lebowitz (ABL) in 1964 [1]. Prior to their theory, measurement in quantum mechanics was taught using the 'von Neumann' type measurements, where after a measurement the quantum state 'collapses' into one of the eigenstates and remains in this eigenstate. This is not time-symmetric, so ABL considered 'evolving' a quantum initial state $|\psi_i\rangle$ forward in time up to a measurement $\hat{A}$, while simultaneously evolving a quantum 'final' state $\langle\psi_f|$ backward in time back to the measurement. This provided a time-symmetric two-state vector formalism for quantum mechanics, where a *weak value* is defined [8]:

$$A_w \equiv \frac{\langle\psi_f|\,\hat{A}\,|\psi_i\rangle}{\langle\psi_f|\,\psi_i\rangle}. \tag{1}$$

The denominator is for normalization. This 'weak value' was claimed by AAV to be the result of such symmetric measurement.

Weak Value Measurement

For over two decades, the time-symmetric approach by ABL seemed to be just a new theory to describe quantum mechanics. However in 1988, Aharonov, Albert, and Vaidman (AAV) applied the time-symmetric two-vector approach to an experiment that could be conducted in the lab [2]. Their title, "How the result of a measurement of a component of the spin of a spin-1/2 particle can turn out to be 100" was peculiar enough that it has since been a source of confusion. The paper suggested a modified Stern-Gerlach experiment (see Figure 1) where electrons with definite spin in one orientation (they called this *'pre-selection'* of the electron state, corresponding to ψ_i in equation (1)), passes through a weak magnetic field (a '*weak*' measurement) to measure the spin z component. Then, the electrons pass through a strong magnetic field oriented so that the spin x was measured. This latter measurement was called a *'post-selection'*, corresponding to ψ_f in equation (1). Their theory predicted that for nearly orthogonal pre- and post-selections, there would be a large deflection of the electrons as if the spin had a value of 100 or more!

The AAV theory as originally written had many errors, and its interpretations have had confusing conclusions (such as complex weak values, negative probabilities, superluminal propagation, and time travel) that are still highly debated today [6, 8]. Duck, Stevenson, and Sudarshan (DSS) provided a nice paper a year after, to correctly state the theory, while confirming the conclusions of AAV, namely that a measurement value can lie outside of the eigenvalue spectrum with the proposed weak value procedure [3]. They also provided corrections to the regions of validity for the AAV theory, one of which was the limit for the weak value itself:

$$A_w \ll \Delta p, \tag{2}$$

where p is the conjugate momentum for the measuring 'pointer,' its deflection/deviation being what is registered for the measurement $\hat{A}$. This shows that $A_w \simeq \Delta p$ is when the AAV theory breaks down, which is also a good approximation for the maximum value for A_w.

Optical Analogue of the Weak Value Spin-1/2 Experiment

DSS went further to provide an equivalent experiment to the spin-1/2 Stern-Gerlach experiment proposed by

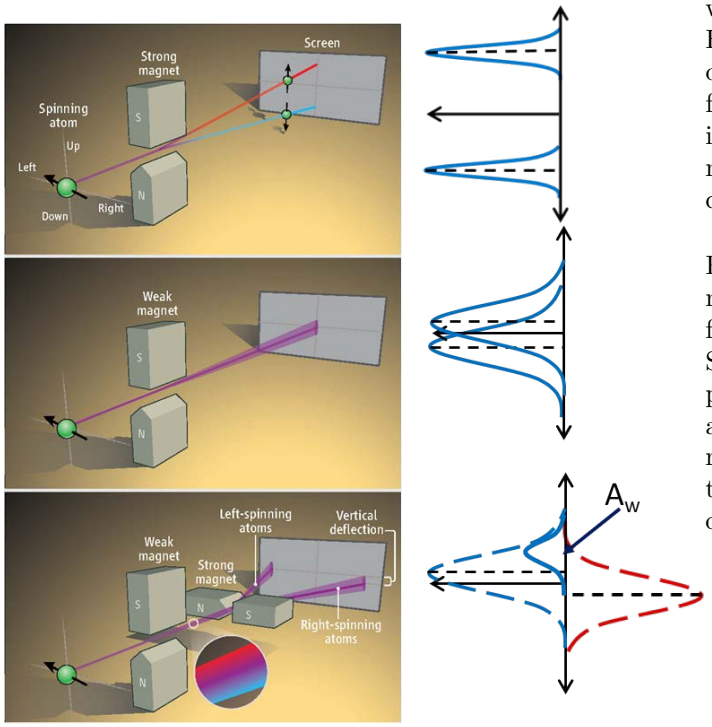

FIG. 1. Spin-1/2 experiment proposed by AAV (Adapted from [6]). **(top)** Von Neumann ('strong') measurement. **(middle)** 'Weak' measurement. **(bottom)** Pre- and post-selections of the spin state. **(right)** Corresponding probability distributions of the wavefunctions of the two separated states. Top shows that the two distinct eigenvalues are clearly separated. Middle shows they are weakly separated (i.e., separation is smaller than the spread). Bottom shows the destructive interference generated from pre- and post-selections, with the resulting distribution being shifted further (centered at A_w, the 'weak value'), albeit with a smaller amplitude. The shift lies within the original spread.

AAV. They proposed a polarized light experiment in which a coherent beam, with Gaussian distribution, is pre-selected in a linearly polarized state, then passes through a birefringent crystal that produces a small displacement between the o ray and the e ray. The birefringent crystal acts as a weak measurement because the separation is small. The beam then is post-selected with a polarizer into a linearly polarized state that is nearly orthogonal to the initial input state, thus providing a large shift in the center of the final Gaussian beam, corresponding to the weak value given in equation (1). The signal is decreased, since the measured intensity I of the final beam follows:

$$I \propto \lambda^2 \delta, \tag{3}$$

where λ is the coupling strength between the birefringent medium and the polarized light, and $1/(2\delta)$ is the spatial width of the initial Gaussian beam. So for weak measurements (small λ coupling), the signal is quite small, which is the 'price' of the large weak value enhancement. However, by repeating the experiment many times, the deflection can be measured to any desired accuracy. In fact, weak value experiments require the experiments being repeated, thus providing an average over repeated measurements, rather than a single measurement, precisely because the measurements are *weak* [6].

The experiment proposed by DSS was conducted by Ritchie et al. in 1991, which was the first 'weak value' measurement [9] (See Figure 2). The beam separation from the birefringent plate used was calculated (from Snell's law and geometry) to be $a = 0.64\mu$m, without any post-selection. For nearly orthogonal linear polarizers P1 and P2 ($\alpha + \pi/2 + 2.2 \times 10^{-2} = \beta$), they showed that the resulting intensity profile was shifted by $A_w = 12\mu$m, 19 times the actual displacement a, albeit with $\sim 10^{-3}$ the original intensity.

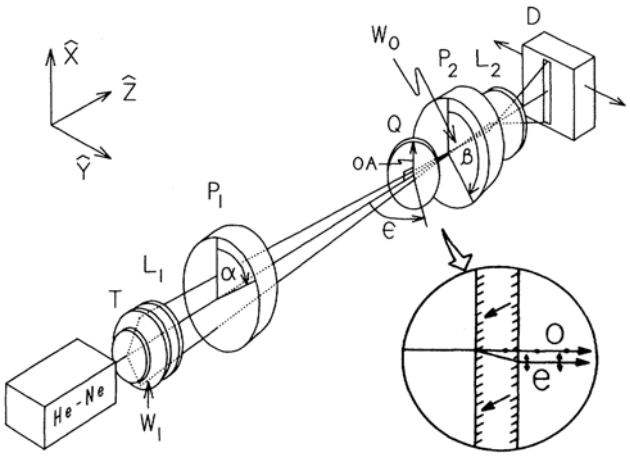

FIG. 2. Experimental setup for Ritchie et al. [9] He-Ne laser is collimated, focused, and polarized at an angle α relative to the x axis by telescope T, lens L1, and polarizer P1, respectively. Birefringent crystalline quartz plate Q with optic axis (OA) aligned along the x axis is located near the laser beam focus. Q spatially separates the ordinary and extraordinary polarization components by a distance small compared to w_0, the focused-beam waist. Polarizer P2, with axis at an angle β with the x axis, post-selects final state. Lens L2 expands image onto photodetector D, which is scanned in the y-direction, measuring intensity I(y). (From [9]) Bottom-right: Displacement of o and e rays after propagation through Q (From [3]).

Understanding Weak Values Intuitively

The optical weak value experiment by DSS and Ritchie et al. used coherent beams with Gaussian distributions to describe the theory. All that is required is for the beam to be coherent across its width. Thus, the experiment and theory are classical and do not require quantum mechanics, nor the weak value measurement formalism of AAV,

although DSS's and Ritchie's works used the AAV formalism [5]. This is the same for the spin-1/2 experiment by AAV, except that the spin of the electrons stems from a quantum mechanical description of matter only. Classically, we can understand the A_w shift in the measurement value using interference. Both pre- and post-selecting polarizers, the birefringent crystal were described by DSS with matrix algebra for the Guassian light beam, using well-known classical formulas in optics. This gives the final, combined field as a function of the transverse direction y:

$$E_f(y) = \cos\beta\cos\alpha\exp[-\delta^2(y-a_1)^2] + \sin\beta\sin\alpha\exp[-\delta^2(y-a_2)^2], \quad (4)$$

where a_1 and a_2 are the two displacements of the o ray and e ray due to the birefringent crystal, which splits the light beam. We see from equation (4) that the final intensity measurement can be written as a sum of two Gaussians each centered about a_1 and a_2. This is what one would expect. These two displacements are the analogue of the two eigenvalues for the spin-1/2 state experiment.

Let us describe the experiment in slightly more detail. Because of the 'weak' measurement, the spreads ($\sim \delta$) of both Gaussian distributions in equation (4) are large and overlap (See right-side of Figure 1). The key to the enhancement is when the post-selection is made to obtain a final state that is nearly orthogonal to the initial state. Then, the two Gaussian beams interefere destructively. We can see this from equation (4), where $\cos\beta \to -\sin\alpha$ and $\cos\alpha \to \sin\beta$ (for small $\alpha > 0$ and $\beta \approx \alpha + \pi/2$), creating a negative sign difference between the two Gaussian parts. Physically the destructive interference occurs because we have selectively removed most of the signal by our orthogonal post-selection. The result is that the final field has a distribution of a single Gaussian beam centered about the weak value A_w as given by AAV. This is shown in Figure 3.

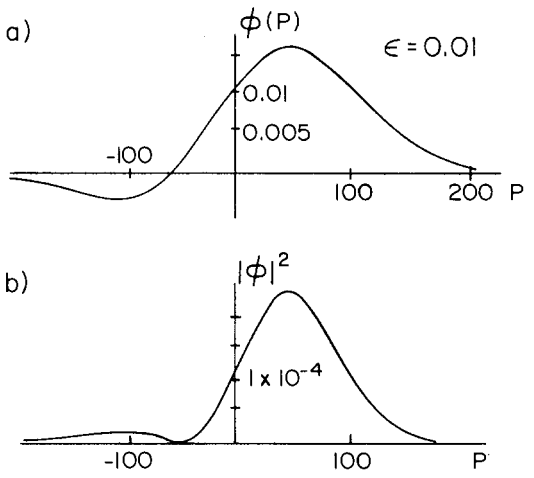

FIG. 3. The final state for nearly orthogonal pre- and post-selected weak value measurements. In momentum space (as opposed to the position space for the optical experiment). ϵ is proportional to how close the (pre-selected) initial and (post-selected) final states are orthogonal (e.g. $\epsilon \sim |\beta - (\alpha + \pi/2)|$). Which side the mean is located, i.e. whether A_w is positive or negative, depends on the sign of ϵ. (a) Final field for the optical DSS experiment, or the measuring device final state for the AAV spin-1/2 experiment. (b) Final intensity, or measuring device probability distribution. (From [3])

NOVEL QUANTUM WEAK VALUE EXPERIMENTS

For over twenty years since the introduction of the theory for weak value measurements, and the initial demonstration of an enhancement effect by Ritchie et al., weak values was not given wide attention. This all changed in 2008 when Hosten and Kwiat used the AAV theory to experimentally demonstrate a $\approx 10^4$ enhancement, which allowed ~ 1Å displacement sensitivity. This was the beginning of an explosion of interest in weak value measurments, with practical application to precision measurement enhancements, as well as measurements of wavefunctions and quantum tests that were previously thought impossible [4–6, 10].

Measuring 1Å from the Spin Hall Effect of Light

In 2008, Hosten and Kwiat measured the 'spin Hall effect of light' (SHEL) for the first time [11]. The Hall effect is where an applied field on transport particles results in a motion perpendicular to the field. The spin Hall effect is due to the interaction of an applied electric field with a spin-polarized current that flows transversely [5]. SHEL is an optical analogue of this effect that was proposed by Onoda et al. [12], and Bliokh and Bliokh [13], where the polarization states of the photons interact with the refractive index gradient of a material. The theory was controversial for 50 years [14], even up until the time of Hosten and Kwiat's experimental verification of the completed theory by Bliokh and Bliokh [15, 16] .

In SHEL, when a beam of light enters a material, at the interface, the beam is displaced. For example, when a horizontally polarized light beam enters a material, due to the change in refractive index, the left-circularly polarized (LCP) and right-circularly polarized (RCP) components (recall linear polarization is a linear combination of LCP and RCP light) experience opposite transverse displacements (not deflections).

The effect of SHEL is quite small, such that this displacement is $\delta \sim 1$Å from SHEL alone. To observe this small effect, Hosten and Kwiat used pre- and post-selections of nearly orthogonal polarization states, before and after the index of refraction material, respectively. The front interface causes the SHEL displacement

which is smaller than the transverse spread of the entering beam, constituting a weak measurement (The second surface was adjusted to be normally incident to the exiting beam to eliminate a secondary SHEL effect). This resulted in an amplification of the small SHEL displacement by nearly $10^4\times$ ('A_w' in Figure 4). Their experimental setup is shown in Figure 4.

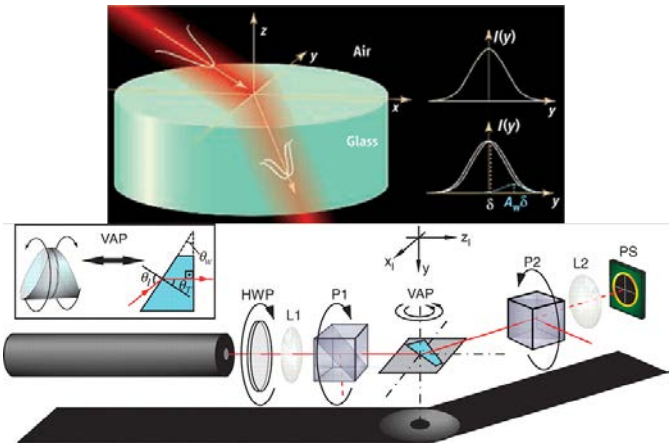

FIG. 4. **(Top-left)** In SHEL, a beam of light separates into two components that are discplaced at the interface, when entering a material with a different index of refraction than the previous medium. **(Top-right)** Gaussian intensity profile of incident beam (top). When weak measurement occurs, the two slightly displaced (by δ) profiles destructively interfere to give a much smaller profile centered about $A_w\delta$. (From [5]). **(Bottom)** Hosten and Kwiat experimental setup. VAP (Variable Angle Prism) generates the weak displacement for SHEL. P1, P2 are nearly orthogonal polarizers, L1, L2 are lenses, HWP is a half-wave plate to adjust incident intensity, and PS is a split photodiode position sensor. (From [11])

Detecting 400 frad Angle Amplification

Shortly after Hosten and Kwiat's 2008 landmark experiment, Dixon, Starling, Jordan, and Howell demonstrated an ultrasensitive beam deflection measurement using interferometers modeled after a weak value measurement scheme [17]. Earlier, the University of Rochester group had shown the usefulness of weak values by demonstrating a sensitive zero or π cross-phase modulation jump from an optical setup combined with Cs atoms, using weak value measurements [18]. However, this next measurement scheme brought much attention due to the high degree of sensitivity possible from the AAV theory, as they had measured 400 femtoradians, which is literally the breadth of a human hair over the distance from the earth to the moon [4, 6, 19]. To be accurate, this experiment can also be described on completely classical grounds, but it was inspired by the quantum mechanical AAV theory [20].

The experiment by Dixon et al. was an implementation of the spin-1/2 experiment by AAV using a Sagnac interferometer with polarized coherent beams (See Figure 5). The polarizing beam splitter sends in a linearly polarized beam, which is separated into two paths (rotating clock-wise or counter-clockwise) by the subsequent beamsplitter. For a perfectly symmetric Sagnac interferometer (without the piezo-driven motor, the half waveplate (HWP), or Soleil-Babinet compensator (SBC)), the output towards the left (and into the CCD or quadrant detector) would be the 'dark port' where no light will exit, due to interference (the 'bright port' is where all the beam exits, and is where the beam initially enters).

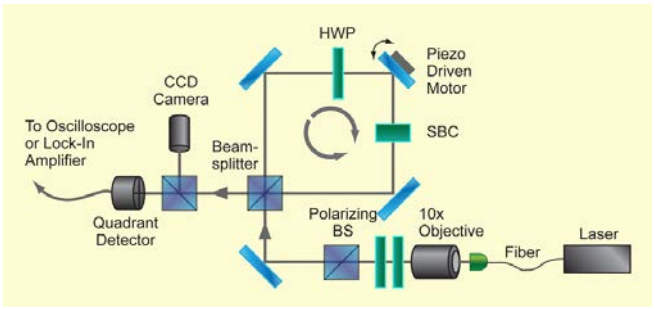

FIG. 5. Experimental setup for Dixon et al.'s weak value measurement of 400 frad (From [19]).

Rotation of the piezo-driven mirror is controlled so as to generate a separation and a deflection for the exiting beam. Thus the beam will exit to the left or right of the optical axis at the exiting port of the beamsplitter, depending on which path the beam traveled in the interferometer. The deflection is measured by a split detector, and gives information about the 'which-path' of the system (clock-wise or counter-clockwise). Since small deflections are made with the piezo motor, this constitutes a weak measurement. The deflection angle was calibrated by measuring the deflection without the beam splitter in the interferometer. By measuring the deflection angle with the beam splitter, and hence the Sagnac interferometric setup, and comparing it to the angle without the beam splitter, an amplification factor was measured. The amplification factor used for the final result was 86.

The combination of the HWP and the SBC generates an asymmetry so that each path obtains a relative phase shift. The HWP changes the horizontal polarization to vertical, and vice versa. The SBC provides a polarization-dependent phase shift ϕ, which can be adjusted. This allows a continual tuning of the phases of the two which-path beams so that the dark port can become the bright port, or any degree of it. The initial pre-selected state is then a linear combination of the two which-path states with relative phases due to the SBC + HWP combination. The final, post-selected state is that linear combination of which-path states that is orthogonal to the initial state for $\phi = 0$. By only detecting at

the original dark port, this post-selection is automatically made. To maximize the weak value 'amplification', ϕ is adjusted to be as close to zero, so that the pre- and post-selected states are nearly orthogonal. It appears that the ideal SBC angle ϕ was 11.5°, limited by the small amount of light exiting the dark port.

The result of the experiment was a 400 ± 200 frad deflection measurement, corresponding to an indirect measurement of 14 ± 7 fm linear travel of the piezo actuator. This was achieved with weak value measurement and a lock-in amplifier. The amplification factor was beam size dependent, it being larger for larger beam sizes. The beam size at the detector was $\sigma = 1240 \pm 50$ μm. The post-selection power was 63 μW from an input power of 3.2 mW, corresponding to a 2% reduction, thus showing the expected diminution of the final signal due to the destructive interference of weak value measurements.

A subsequent study by the same authors [21] provided the first careful accounting of the signal-to-noise ratio (SNR) of weak value amplification (WVA) [22]. They showed that the SNR for WVA was larger than standard detection schemes that produce the same beam size on the detector. However, the SNR for WVA was the same order as when a lens is used to focus the beam onto a split detector. However, there are significant advantages for WVA. They are that the technical noise is reduced by the square root of the post-selection probability ($\sin^2(\phi/2)$ for Ref. 17), low power detectors can be used with high power lasers, and the ulitimate limit can be achieved with a large beam radius. Compared to the deflection without WVA or a focusing lens, a factor of 54 improvement in SNR was produced experimentally.

Other Significant Weak Value Experiments

There have been many more experiments utilizing the AAV theory since Hosten and Kwiat's paper for SHEL. Lundeen and Steinberg used weak values to 'resolve' Hardy's paradox, where electrons and positrons go through two interferometers that overlap [23] (See Figure 6). The paradox is that both the electrons and/or the positrons will come out of the dark port sometimes, due to their interference from the overlapping region, *but* when the two particles overlap, they should have annihilated each other! Using simultaneous weak measurements with an optical analogue experiment, Lundeen and Steinberg showed that the probability of finding the electron in its overlapping path and the positron in the nonoverlapping path, and vice versa, are both 100%, thus 'resolving' the pardox. However, this totals 200%, but this is also not a problem since the probability of finding both particles in the nonoverlapping paths is -100%, allowing the net probabiliy to be exactly 100%. The price to pay is to accept negative probabilities [6].

Perhaps one of the most fascinating experiments using weak values came from two groups in June 2011, where single photon wavefunctions were directly measured [24, 25] (See Figure 7). The trick was to weakly measure the momentum or position and strongly measure the other conjugate variable. Of course this doesn't violate our standard notion of quantum mechanical measurements and preserves the Heisenberg uncertainty principle between two conjugate observables, because the final trajectories are the results of averaging many measurements. Nonetheless, these experiments have made many physicists rethink our understanding of quantum mechanical wavefunctions [10].

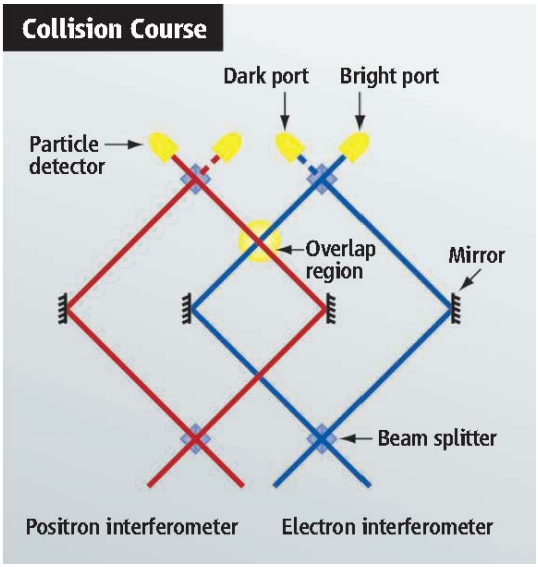

FIG. 6. Hardy's paradox (From [6]).

Finally, in 2012, a weak value experiment by the Steinberg group even went so far as to question one of the fundamental principles of quantum mechanics- the Heisenberg uncertainty principle [26]. As originally formulated by Heisenberg himself, the uncertainty principle stated that a measurement of the position of a particle by a photon imparts a momentum disturbance to the particle from the photon-particle scattering event, and is larger for more precise measurements (smaller photon wavelengths). This original formulation (called measurement-disturbance relationship (MDR) by [26]) is not the same as what is proved mathematically in modern textbooks. The former was shown to be less general and mathematically incorrect. The modern version, commonly referred to as the Heisenberg uncertainty principle (HUP) refers to the uncertainties intrinsic in the quantum state, not to the precision and disturbance relationship. For arbitrary observables $\hat{A}$ and $\hat{B}$, where $\Delta\hat{A} = \sqrt{<\hat{A}^2> - <\hat{A}>^2}$, HUP is written as:

$$\Delta\hat{A}\Delta\hat{B} \geq \tfrac{1}{2}\left|<[\hat{A},\hat{B}]>\right|. \qquad (5)$$

The original Heisenberg's measurement-disturbance rela-

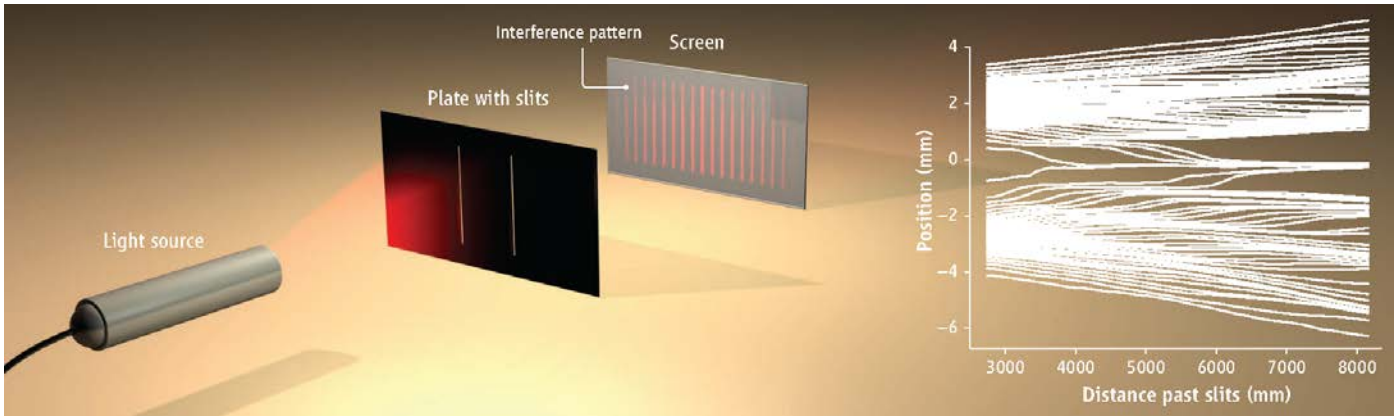

FIG. 7. Phase-space measurement of single photons through a two-slit setup by Steinberg and colleagues [25]. (From [6]).

tionship (MDR) is written as:

$$\epsilon(\hat{A})\eta(\hat{B}) \geq \tfrac{1}{2}\left|<[\hat{A},\hat{B}]>\right|, \tag{6}$$

where $\epsilon(\hat{A})$ is the measurement precision, and $\eta(\hat{B})$ is the induced disturbance from the measurement. Ozawa proved a corrected relationship that includes both the standard deviation and the precision + disturbance combination [27]:

$$\epsilon(\hat{A})\eta(\hat{B}) + \epsilon(\hat{A})\Delta\hat{B} + \eta(\hat{B})\Delta\hat{A} \geq \tfrac{1}{2}\left|<[\hat{A},\hat{B}]>\right|, \tag{7}$$

The experimental setup by the Steinberg group to measure a single photon is shown in Figure 8. The $\hat{X}$ and $\hat{Z}$ polarization observables were used, yielding the right-hand side (RHS) of equations (6) and (7) to be $|<\hat{Y}>|$. The system (the polarization of a single photon) was prepared to maximize RHS so that the MDR inequality (equation (6)) could be violated. A probe interacts with the system weakly, then is strongly measured (shaded area of Figure 8 (a)). The system and probe become entangled through this interaction ('measurement apparatus' (MA)), disturbing the system. The system is also weakly measured prior to the MA. The precision $\epsilon(\hat{A})$ was defined to be the root mean square (RMS) difference between the value of $\hat{A}$ on the system before the interaction, and the value of it read out on the probe. The disturbance $\eta(\hat{B})$ was then defined to be the RMS difference between the value of $\hat{B}$ on the system before and after the MA.

The results of the experiment are shown in Figure 9. The bottom plot shows that the MDR relation is violated, while the Ozawa relationship holds. Thus, Rozema and the Steinberg group showed experimentally, what was previously thought impossible to demonstrate [26], that the original Heisenberg formulation of the uncertainty principle is incorrect.

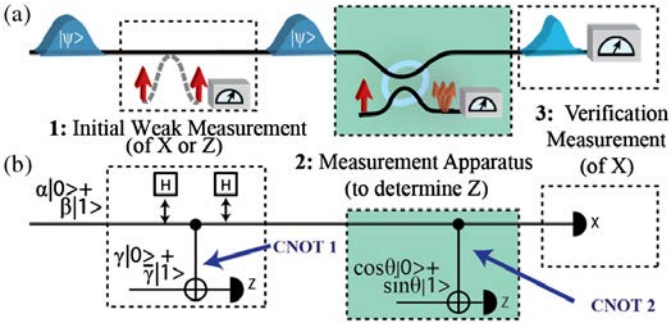

FIG. 8. Weak measurement experiment testing the Heisenberg uncertainty principle as originally proposed by Lund and Wiseman [28], and conducted by Rozema et al. (Steinberg group) [26] (a) General method to measure precision and disturbance, where a weak measurement is made before the measurement apparatus, followed by a strong measurement. (b) Quantum circuit application for a qubit system. (From [26]).

WEAK SIGNAL AMPLIFICATION TECHNIQUES IN CHEMISTRY

In the field of chemistry, *chiral* molecules are molecules with non-superimposable mirror images and are often studied because probing the two left-handed and right-handed *enantiomers* provide three-dimensional stereoscopic information. In addition, producing the right enantiomer is important for pharmaceutical manufacturing since drugs with the wrong chirality can be poisonous.

Left- or right-handed enantiomers have different indices of refraction for left- or right-circularly polarized (LCP or RCP) light. Thus, when a beam traverses a chiral medium, its polarization rotates, or its ellipticity changes, due to the difference in the real part and imaginary part of the index of refraction, respectively. The former is called *optical rotatory dispersion (ORD)*, and the latter is called *circular Dichroism (CD)*. These quantities are directly proportional to the differential index of refraction (real part) and the differential absorption be-

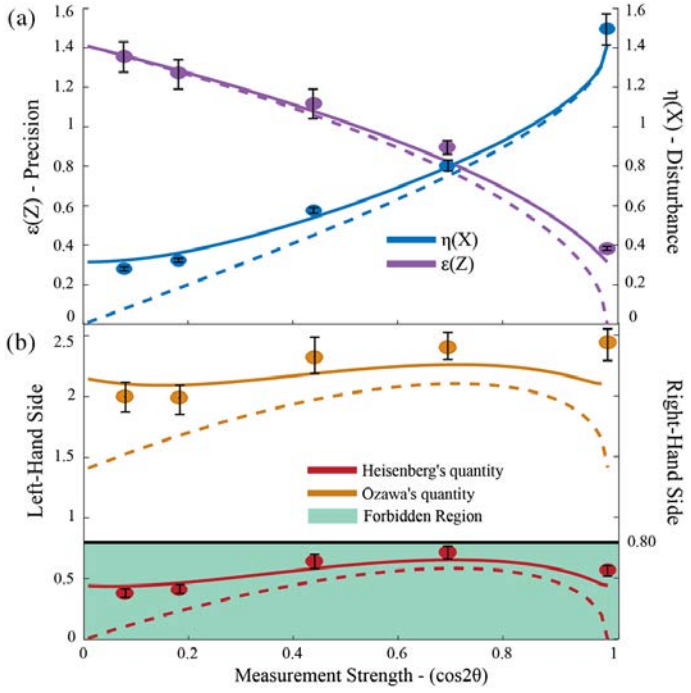

FIG. 9. Experimental results of testing the Heisenberg uncertainty principle, by Rozema et al. using $\hat{X}, \hat{Z}$ polarizations of light [26]. (a) Precision and induced disturbance. (b) Plot of left-hand side of the Heisenberg and Ozawa relations in equations (6) and (7). respectively. Right-hand side is $|<\hat{Y}>|$ polarization, and was measured to be 0.80±0.02. Heisenberg's MDR quantity lies below $|<\hat{Y}>|$, a clear violation of the original Heisenberg uncertainty principle in equation (6). However, Ozawa's relation is shown to still hold true. (From [26]).

tween LCP and RCP light, respectively.

To measure the ability to selectively excite one enantiomer over the other (called *optical enantioselectivity*), thereby quantifying the chirality of a sample, a quantity called the dissymmetry factor is used. It is defined as:

$$g = \frac{A^+ - A^-}{(A^+ + A^-)/2}, \tag{8}$$

where A^+, A^- are the absorption rates for 'left-handed' (+) and 'right-handed' (−) fields, respectively. When LCP and RCP lights are used, we denote this as $g \to g_{\text{CPL}}$. For such case, the dissymmetry factor defined in equation (8) is the CD divided by the average absorption, and is a proper criterion for determining whether the CD is measurable for a particular absorption band, given the available instrumental sensitivity [29]. The dissymmetry factor is typically quite small, with a range of 10^{-6}–10^{-2}, the lower end corresponding to vibrational spectrum, and the upper end for electronic spectrum. Many in the field of chemistry have thus attempted to measure or enhance this small signal, contributing to novel methods for doing just that. Here we discuss two methods.

Enhanced Optical Enantioselectivity- 'Superchiral' Fields

In 2010 and 2011, Tang and Cohen proposed and demonstrated one method to enhance optical enantioselectivity with a 11× enhancement (g/g_{CPL}) by using a standing wave chiral field (SWCF) instead of the typical circularly polarized light (CPL) [30, 31]. Their proposal was ingenious in its simplicity and creativity. They simply placed a mirror with reflectivity R to reflect the CPL, creating a standing wave instead. At the electric field minimum they placed their chiral sample, at which point their theory showed an enhancement in the dissymmetry factor (See Figure 10). To measure g_{CPL}, they used a sample without a mirror, and measured the differential absorption for LCP and RCP light. To measure the enhanced g, they used a sample with a mirror, and measured the differential absorption of the 'left'- and 'right'-handed standing waves, created by an LCP incident light or an RCP incident light. Because $R < 1$, these two SWCFs are either more left-handed or more right-handed than the other, thereby providing a nonzero dissymmetry factor.

The original theory by Tang and Cohen showed an infinite enhancement for a perfectly reflecting mirror, which was corrected by Choi and Cho by including the omitted magnetic field component properly [32].

$$\frac{g}{g_{\text{CPL}}} \simeq \frac{cC}{2n\omega\left[\langle U_e\rangle_t + \gamma\langle U_b\rangle_t\right]} \Rightarrow \frac{1-R}{(1+R)(1+\gamma)+2\sqrt{R}(\gamma-1)\cos(2kz)}, \tag{9}$$

where C is the 'optical chirality' Tang and Cohen used to quantify the chirality of the field, R is the reflectivity, ω is the angular frequency, n is the average index of refraction of the material, $\langle U_e\rangle_t$ and $\langle U_b\rangle_t$ are the time-averaged electric and magnetic field energy densities, respectively. z is the position along the propagation axis of the field, k is its wave vector, and finally $\gamma \propto$ (magnetic susceptibility)/(electric polarizability) $\approx 10^{-6} - 10^{-4}$ and hence is a property of the sample used. The right-hand side of the right-arrow is for the SWCF case specifically, while the left-side is general. The corrected formula showed that there is an enhancement when the electric field is at a minimum ($\cos(2kz) = 1$). At this nodal region, the enhancement has the general shape shown in Figure 11 as a function of R. The chiral sample used fixes the shape, and thus determines the maximum enhancement that can be achieved, which ranges from 15× to 500× for realistic samples. Although Tang and Cohen originally devised their 'superchiral' field in an attempt to increase the chiral nature of their newly engineered field, the optical chirality C that quantifies this is actually constant in space and time for the SWCF. The enhancement they observed comes

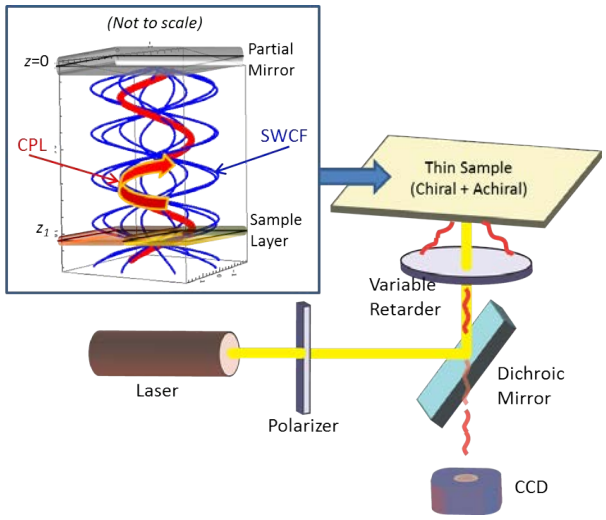

FIG. 10. Tang and Cohen experimental setup [31]. Experimental setup for enhancement using a standing-wave chiral field (SWCF). Two samples used, one with mirror coating, and one without, to measure g, g_{CPL} respectively. The thin sample has both a chiral and an achiral layer on a 170μm thick glass coverslip. Laser light was polarized to avoid distortion from the dichroic. The variable retarder converted the linearly polarized light alternately into left- and right-circularly polarized light. Fluorescence was imaged on a charge-coupled device camera (CCD), after being separated from excitation light by the dichroic mirror and a filter (not shown).
(Inset) Electric fields of SWCF compared to circularly polarized light (CPL) interacting with the thin sample chiral/achiral layer ('sample layer'), obtained from the experimental values (R=0.72, 543.5 nm wavelength). The CPL (red) is left-CPL, traveling in the $-z$ direction. When reflected by the mirror, a standing wave (SWCF; blue) is created. The CPL shown is for a fixed time, but the SWCF shown is a sum of eight 1/8 periods. The fields shown are over a propagation distance of $\sim 1.2\mu\mathrm{m}(z_1 = 1\mu\mathrm{m})$. This illustrates that the chiral/achiral sample layer can spatially fit inside a nodal electric field region for the SWCF. (The mirror and sample layer were 19 nm, 10 nm thick, respectively)

from placing the chiral sample at the electric field node, and is maximized when $[\langle U_e\rangle_t + \gamma \langle U_b\rangle_t]$ is minimized in the denominator of equation (9), *much like* when the weak value is maximized by finding a nearly zero denominator term in equation (1). For the 'superchiral' field case, due to conservation of energy, the denominator never becomes zero but achieves its minimum when $\langle U_e\rangle_t \sim \gamma \langle U_b\rangle_t$ [32]. This condition is close to the nodal electric field region ($\langle U_e\rangle_t = 0$) since γ is so small. This implies that the signal obtained is also very small, similar to weak values. On another note, one could search for samples with smaller γ to obtain higher enhancements, but the signal decreases faster than the increase in enhancement, making this search not as fruitful as one would hope.

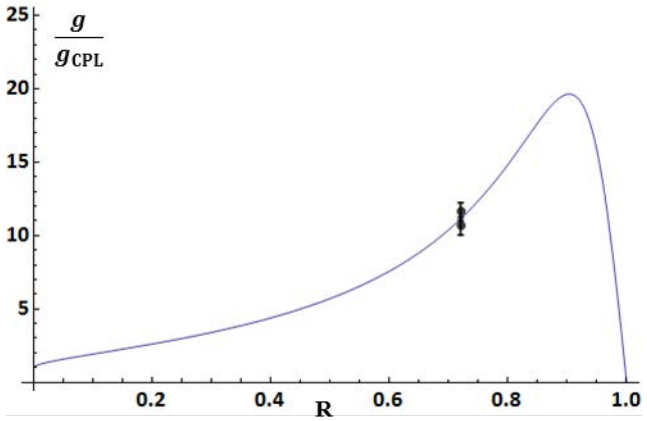

FIG. 11. Dissymmetry factor enhancement of a SWCF field over CPL fields for [31], as a function of the reflectivity R of the mirror used. Plot is for the chiral sample that was used, at the electric field node, and for $\gamma = 0.00065$ fit to the experimental data (points with error bars).

Quasi-null Ellipsometric Chiroptical Spectroscopy

Published in 1985, the Kliger group (Lewis et al. [33]) demonstrated a method to measure protein dynamics through measurement of circular dichroism on a nanosecond time scale. Their method allowed time resolution of CD to be enhanced by a factor of 10^6. They took advantage of the fact that a chiral sample will change the ellipticity of elliptically polarized light. First they sent a linearly polarized light and converted it to either left-elliptically polarized (LEP) or right-elliptically polarized (REP) light. They then measured the absorption of a chiral sample from the (LEP) light or the (REP) light. The differential CD signal was obtained by passing it through a linear polarizer that was perpendicular to the original linear polarizer. This method was later called *'quasi-null ellipsometric chiroptical spectroscopy.'* It allowed for a 10^3 enhancement of the dissymmetry factor, compared to standard measurements, which corresponds to the same increase for the SNR. Since time resolution goes as the square of the SNR, this then corresponds to the 10^6 enhancement.

In 2009, Helbing and Bonmarin [34], Rhee and the Cho group [35] adapted Kliger's technique to measure both the vibrational CD and ORD signals. Vibrational signals are much smaller than that for the electronic spectra, with dissymmetry factors being $(10^{-6} - 10^{-4})$ compared to $(10^{-3} - 10^{-2})$ for the electronic transition signals. The Cho group combined heterodyned detection with Kliger's method, and with femtosecond pulses to probe the chirality of the sample. Conventional vibrational CD spectroscopy requires hours of data collection because of the small signal. However, Cho's technique was able to collect the chiral data almost instantaneously, opening up the possibility of the probing of molecular and biological

dynamics efficiently. Later, the Cho group showed the ability to conduct these measurements on a single-shot basis [36, 37].

Figure 12 shows the experimental setup for the 2009 Rhee and Cho work. The pulse is initially linearly polarized before propagating through the chiral sample. The chiral sample changes each circular polarized component into elliptically polarized lights by both optical rotation and differential absorption (through CD). The elliptically polarized light is then filtered through an orthogonal linear polarizer which selects the chiral signal, at the expense of a smaller final signal. This is then combined with a heteroduned signal separated from the original beam.

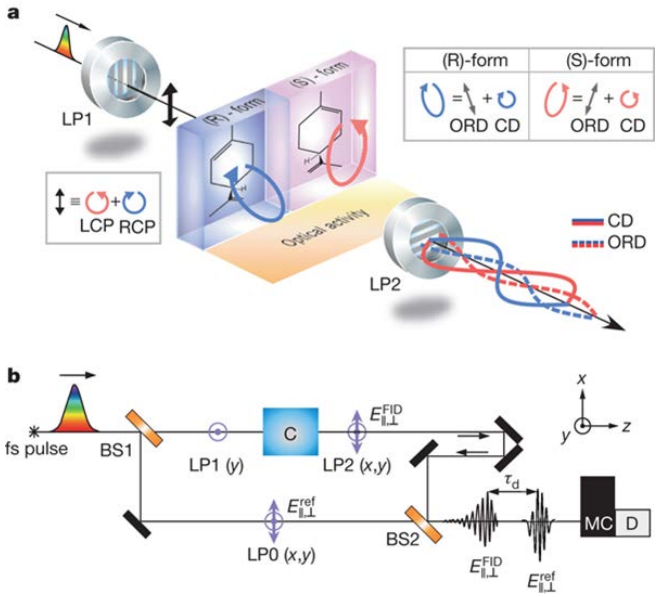

FIG. 12. (a) Coherent pulse goes through a chiral sample. LP1 and LP2 are orthogonal linear polarizers. The outgoing left- and right-handed fields are out of phase with each other. (b) Sketch of the setup for Fourier transform spectral interferometry. BS are beamsplitters that separate and recombine the probe pulse and the heterodyned pulse. LP's are linear polarizers, and the final combined field is dispersed by a monochromator (MC) and detected by detector D. (From [35])

The enhancements of these small signals can be described by the AAV theory for weak value measurement [38]. Thus, Kliger's work provides an example of a 'weak value' experiment that was performed prior to the AAV formalism, and described classically.

CONCLUSION

An overview of the weak value measurement theory by AAV was provided, along with significant experiments that have verified some of their conclusions. These theory and experiments have opened up new insights into high-precision measurements, have opened up new measurement techniques previously thought impossible in quantum mechanics, and continues to surprise many with controversial and interesting viewpoints. A few selected enhancement techniques used in the field of chemistry for chiral signals that are small have been introduced as well. We can see that these techniques in chemistry have similarities with weak value measurements, some being that the enhancement is for small signals, and is obtained by throwing away most of the signal. In fact, the quasi-null ellipsometric chiroptical spectroscopy developed by Kliger's group in 1985 can be written in the weak value formalism. We can look forward to developments in the future for improved measurements in both physics and chemistry as scientists from both share and collaborate on ideas that have served both fields so well. Some have already begun connecting chiral fields and weak value measurments [14, 39], and a minireview containing experiments described here will be published in Chemical Science by the author and collaborators [7].

The author would like to thank Professor John Howell, Professor Minhaeng Cho, Dr. Hanju Rhee, and Dr. David Starling for their insights and discussions that helped to formulate this paper. The author was supported by an IGERT Fellowship from the National Science Foundation. Many figures were taken from the published sources, as noted, since this paper is intended for academic purposes.

* joschoi@optics.rochester.edu

[1] Yakir Aharonov, Peter G. Bergmann, and Joel L. Lebowitz. Time symmetry in the quantum process of measurement. *Physical Review*, 134(6B):B1410–B1416, 1964.

[2] Y. Aharonov, D. Z. Albert, and L. Vaidman. How the result of a measurement of a component of the spin of a spin-1/2 particle can turn out to be 100. *Physical Review Letters*, 60(14):1351–1354, 1988.

[3] I. M. Duck, P. M. Stevenson, and E. C. G. Sudarshan. The sense in which a weak measurement of a spin-1/2 particles spin component yields a value 100. *Physical Review D*, 40(6):2112–2117, 1989.

[4] Y. Aharonov, S. Popescu, and J. Tollaksen. A time-symmetric formulation of quantum mechanics. *Physics Today*, 63(11):27–32, 2010.

[5] K. J. Resch. Physics - amplifying a tiny optical effect. *Science*, 319(5864):733–734, 2008.

[6] Adrian Cho. Physics furtive approach rolls back the limits of quantum uncertainty. *Science*, 333(6043):690–693, 2011.

[7] Hanju Rhee, Joseph S. Choi, David Starling, John Howell, and Minhaeng Cho. Enhancement methods in chiroptical spectroscopy, optical enantioselectivity, and weak value measurement. (To be published).

[8] Yakir Aharonov and Lev Vaidman. The two-state vector formalism of qauntum mechanics: an updated review.

arXiv:quant-ph/0105101v2.

[9] N. W. M. Ritchie, J. G. Story, and R. G. Hulet. Realization of a measurement of a weak value. *Physical Review Letters*, 66(9):1107–1110, 1991.

[10] Onur Hosten. Quantum physics how to catch a wave. *Nature*, 474(7350):170–171, 2011.

[11] Onur Hosten and Paul Kwiat. Observation of the spin hall effect of light via weak measurements. *Science*, 319(5864):787–790, 2008.

[12] M. Onoda, S. Murakami, and N. Nagaosa. Hall effect of light. *Physical Review Letters*, 93(8):083901, 2004.

[13] K. Y. Bliokh and Y. P. Bliokh. Topological spin transport of photons: the optical magnus effect and berry phase. *Physics Letters A*, 333(3-4):181–186, 2004.

[14] Y. Gorodetski, K. Y. Bliokh, B. Stein, C. Genet, N. Shitrit, V. Kleiner, E. Hasman, and T. W. Ebbesen. Weak measurements of light chirality with a plasmonic slit. *Physical Review Letters*, 109(1):013901, 2012.

[15] K. Y. Bliokh and Y. P. Bliokh. Conservation of angular momentum, transverse shift, and spin hall effect in reflection and refraction of an electromagnetic wave packet. *Physical Review Letters*, 96(7):073903, 2006.

[16] K. Yu Bliokh and Yu P. Bliokh. Polarization, transverse shifts, and angular momentum conservation laws in partial reflection and refraction of an electromagnetic wave packet. *Physical Review E*, 75(6):066609, 2007.

[17] P. B. Dixon, D. J. Starling, A. N. Jordan, and J. C. Howell. Ultrasensitive beam deflection measurement via interferometric weak value amplification. *Physical Review Letters*, 102(17):173601, 2009.

[18] Ryan M. Camacho, P. Ben Dixon, Ryan T. Glasser, Andrew N. Jordan, and John C. Howell. Realization of an all-optical zero to pi cross-phase modulation jump. *Physical Review Letters*, 102(1):013902, 2009.

[19] S. Popescu. Weak measurements just got stronger. *Physics*, 2:32, 2009.

[20] John C. Howell, David J. Starling, Ben P. Dixon, Praveen K. Vudyasetu, and Andrew N. Jordan. Interferometric weak value deflections: Quantum and classical treatments. *Physical Review A*, 81(3):3, 2010.

[21] David J. Starling, P. Ben Dixon, Andrew N. Jordan, and John C. Howell. Optimizing the signal-to-noise ratio of a beam-deflection measurement with interferometric weak values. *Physical Review A*, 80(4):041803, 2009.

[22] Aephraim M. Steinberg. Quantum measurement: A light touch. *Nature*, 463(7283):890–891, 2010.

[23] J. S. Lundeen and A. M. Steinberg. Experimental joint weak measurement on a photon pair as a probe of hardy's paradox. *Physical Review Letters*, 102(2):4, 2009.

[24] Jeff S. Lundeen, Brandon Sutherland, Aabid Patel, Corey Stewart, and Charles Bamber. Direct measurement of the quantum wavefunction. *Nature*, 474(7350):188–191, 2011.

[25] Sacha Kocsis, Boris Braverman, Sylvain Ravets, Martin J. Stevens, Richard P. Mirin, L. Krister Shalm, and Aephraim M. Steinberg. Observing the average trajectories of single photons in a two-slit interferometer. *Science*, 332(6034):1170–1173, 2011.

[26] Lee A. Rozema, Ardavan Darabi, Dylan H. Mahler, Alex Hayat, Yasaman Soudagar, and Aephraim M. Steinberg. Violation of heisenberg's measurement-disturbance relationship by weak measurements. *Physical Review Letters*, 109(10):100404, 2012.

[27] Masanao Ozawa. Universally valid reformulation of the heisenberg uncertainty principle on noise and disturbance in measurement. *Physical Review A*, 67(4):042105, 2003.

[28] A. P. Lund and H. M. Wiseman. Measuring measurement-disturbance relationships with weak values. *New Journal of Physics*, 12:093011, 2010.

[29] Laurence Barron. *Molecular Light Scattering and Optical Activity*. Cambridge University Press, Cambridge, UK, 2 edition, 2004.

[30] Yiqiao Tang and Adam E. Cohen. Optical chirality and its interaction with matter. *Physical Review Letters*, 104(16):163901, 2010.

[31] Yiqiao Tang and Adam E. Cohen. Enhanced enantioselectivity in excitation of chiral molecules by superchiral light. *Science*, 332(6027):333–336, 2011.

[32] Joseph S. Choi and Minhaeng Cho. Limitations of a superchiral field. *Physical Review A*, 86(6):063834, 2012.

[33] J. W. Lewis, R. F. Tilton, C. M. Einterz, S. J. Milder, I. D. Kuntz, and D. S. Kliger. New technique for measuring circular-dichroism changes on a nanosecond time scale - application to (carbonmonoxy)myoglobin and (carbonmonoxy)hemoglobin. *Journal of Physical Chemistry*, 89(2):289–294, 1985.

[34] Jan Helbing and Mathias Bonmarin. Vibrational circular dichroism signal enhancement using self-heterodyning with elliptically polarized laser pulses. *Journal of Chemical Physics*, 131(17):174507, 2009.

[35] Hanju Rhee, Young-Gun June, Jang-Soo Lee, Kyung-Koo Lee, Jeong-Hyon Ha, Zee Hwan Kim, Seung-Joon Jeon, and Minhaeng Cho. Femtosecond characterization of vibrational optical activity of chiral molecules. *Nature*, 458(7236):310–313, 2009.

[36] Intae Eom, Sung-Hyun Ahn, Hanju Rhee, and Minhaeng Cho. Broadband near uv to visible optical activity measurement using self-heterodyned method. *Optics Express*, 19(10):10017–10028, 2011.

[37] Intae Eom, Sung-Hyun Ahn, Hanju Rhee, and Minhaeng Cho. Single-shot electronic optical activity interferometry: Power and phase fluctuation-free measurement. *Physical Review Letters*, 108(10):103901, 2012.

[38] Minhaeng Cho. Connection between chiroptical signal enhancements and weak measurements. (To be published).

[39] Konstantin Y. Bliokh, Aleksandr Y. Bekshaev, and Franco Nori. Dual electromagnetism: helicity, spin, momentum and angular momentum. *New Journal of Physics*, 15:033026, 2013.